Ultrafast Spectroscopy of Excitons in Single-Walled Carbon Nanotubes

O. J. Korovyanko,[1] C.-X. Sheng,[1] Z. V. Vardeny,[1] A. B. Dalton,[2] and R. H. Baughman[2]
[1]*Department of Physics, University of Utah, Salt Lake City, Utah 84112, USA*
[2]*Nano Tech Institute, University of Texas at Dallas, Richardson, Texas 75083, USA*
(Received 29 July 2003; published 9 January 2004)

We studied the femtosecond dynamics of photoexcitations in films containing semiconducting and metallic single-walled carbon nanotubes (SWNTs), using various pump-probe wavelengths and intensities. We found that confined excitons and charge carriers with subpicosecond dynamics dominate the ultrafast response in semiconducting and metallic SWNTs, respectively. Surprisingly, we also found from the exciton excited state absorption bands and multiphoton absorption resonances in the semiconducting nanotubes that transitions between subbands are allowed; this unravels the important role of electron-electron interaction in SWNT optics.

DOI: 10.1103/PhysRevLett.92.017403 PACS numbers: 78.47.+p, 72.20.Jv, 78.55.Kz, 78.67.Ch

Because of the nanometer scale diameter and extended dimension along the tube, single-walled carbon nanotubes (SWNTs) are considered to be quasi-one-dimensional (1D) solids [1]. Depending on their chirality, SWNTs can be either semiconducting or metallic [2]. In recent years, much effort has been devoted to studying Coulomb interaction in quasi-1D electronic systems [3]. Peierls instability in electron-phonon 1D metal [4] and large binding energy excitons in 1D semiconductors [5] are two well-known examples of electronic confinement in 1D systems. Nevertheless, the role of electron-electron (*e-e*) interaction in SWNTs has not yet been studied in detail. Recent improvements in sample preparation led to the discovery of fluorescence in isolated SWNTs [6], and the realization that *e-e* interaction in SWNTs is important [7–9]. In particular, it is clear that excitons are responsible for the measured fluorescence [6], and that the use of tight binding approximation to calculate the electronic band structure cannot account for various features seen in the optical absorption spectrum of SWNTs [7–9].

In this Letter, we provide further experimental evidence for the importance of *e-e* interaction in SWNTs. We measured the ultrafast dynamics of photoexcitations in films of SWNTs that contain both semiconducting (S) and metallic (M) nanotubes (NTs). From the transient photoinduced absorption bands, multiphoton absorption resonances, and polarization memory dynamics, we conclude that the primary photoexcitations in S NTs are confined *excitons* with allowed optical transitions between subbands; these transitions are strictly forbidden in the tight binding approximation. In contrast, the ultrafast photoresponse in M NTs is determined by hot carrier dynamics.

We used the femtosecond two-color pump-probe correlation technique with linearly polarized light beams in a broad spectral range from 0.6 to 2.6 eV, and pump intensities (I) ranging from 0.1 to 3000 μJ/cm^2. For the high-intensity measurements, we used a titanium-sapphire laser amplifier system followed by an optical parametric amplifier having 100 fs pulses at photon energies of 1.55 eV and from 0.7 to 1.1 eV, as well as frequency-doubled pulses from 1.8 to 2 eV. Four percent of the output was split to generate white light supercontinuum for the probe beam in the spectral range from 1.2 to 2.7 eV. For the low-intensity measurements, we used a titanium-sapphire pumped optical parametric oscillator with 100 fs pulses, which extended the transient photomodulation (PM) spectral range into the mid-IR from 0.56 to 0.73 eV and 0.84 to 1.02 eV. The transient PM signal, $[\Delta T(t)/T]$ is the fractional change in transmission, which is negative for photoinduced absorption (PA) and positive for photobleaching (PB). To obtain the transient polarization memory, $P(t)$, we measured $\Delta T/T$ for pump-probe polarizations either parallel (ΔT_p) or perpendicular (ΔT_{pe}) to each other, and calculate $P(t) = (\Delta T_p - \Delta T_{pe})/(\Delta T_p + \Delta T_{pe})$.

The SWNTs were grown using a modified gas phase process (HiPco), and were supplied by Carbon Nanotechnologies Inc. The raw material was initially dispersed in deionized water using an anionic surfactant lithium dodecyl sulfate. SWNT thin films were subsequently prepared on silica substrates by successive dip coating followed by a ten-hour bake at 70 °C. The films were annealed for 5 h in Ar atmosphere at 600 °C. The NTs contain approximately 12%–15% by weight Fe catalyst but are otherwise relatively free of carbonaceous impurities commonly associated with other production methods. Atomic force microscopy and resonant Raman spectroscopy suggested an average NT length of ~400 nm, and a diameter distribution ranging from 0.8 to 1.2 nm.

A typical absorption spectrum of the SWNT films is shown in the Fig. 1 inset. Three prominent absorption bands and a shoulder are seen at 0.8 eV (A), 1.35 eV (B), 1.9 eV (C), and 2.5 eV (D), respectively, which are superimposed onto broad background absorption [10,11]. Bands A, B, and D were previously assigned [1,11] to the inhomogeneously broadened interband optical transitions in S NTs from various valence subbands to their respective conduction subbands with the *same* index, m; namely

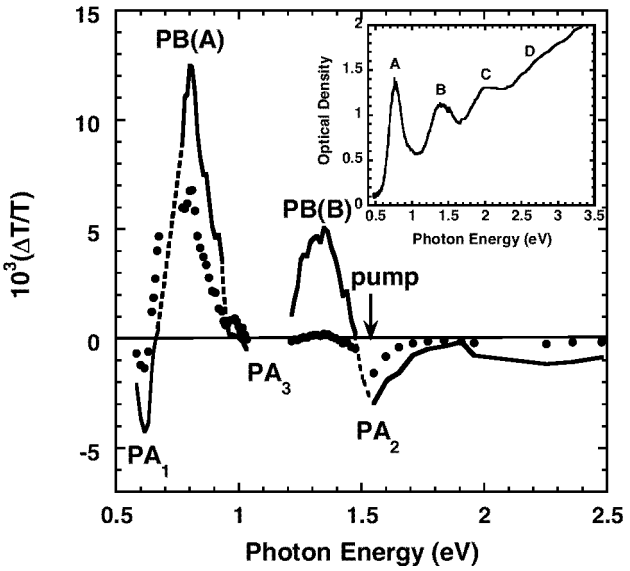

FIG. 1. The transient PM spectra of a SWNT film at $t = 0$ (full line) and $t = 500$ fs (dotted line) excited at 1.55 eV; the dashed line is a guide to the eye. Various PB and PA bands are assigned. The inset shows the absorption spectrum of the film, where bands A to D are assigned.

$m = 1$, 2, and 3, respectively [Fig. 2(a)]. On the contrary, band C at 1.9 eV was assigned [1,11] to the $m = 1$ interband transition in M NTs.

The transient PM spectra of a SWNT film at 300 K excited at 1.55 eV and measured at delay times $t = 0$ and $t = 500$ fs, respectively, are shown in Fig. 1; the spectra contain contributions from both the high- and low-intensity laser systems, which were normalized to each other in the mid-IR spectral range. The PM spectra reveal two PB bands that peak at 0.79 [PB(A)] and 1.35 eV [PB(B)], respectively; two PA bands with peaks around 0.6 (PA_1) and 1.6 eV (PA_2), and the threshold of a third PA band (PA_3) at 1.03 eV Since the PB bands correspond to absorption bands A and B of S NT (Fig. 1 inset), we assign them as photobleaching of these two bands. The PB is due to either k-space state filling [12] or Q-space filling [13], depending on whether carriers [Fig. 2(a)] or excitons (Fig. 2(b)] are photogenerated at $t = 0$. From the transient dynamics seen in Fig. 3, it is clear that PB(B) decays much faster than PB(A), in agreement with previous literature [10]. We thus explain PB(B) fast decay as due to photoexcitation thermalization from $m = 2$ to $m = 1$ subbands. The transient PA, on the other hand, was interpreted [10] as due to transient dynamics of the absorption

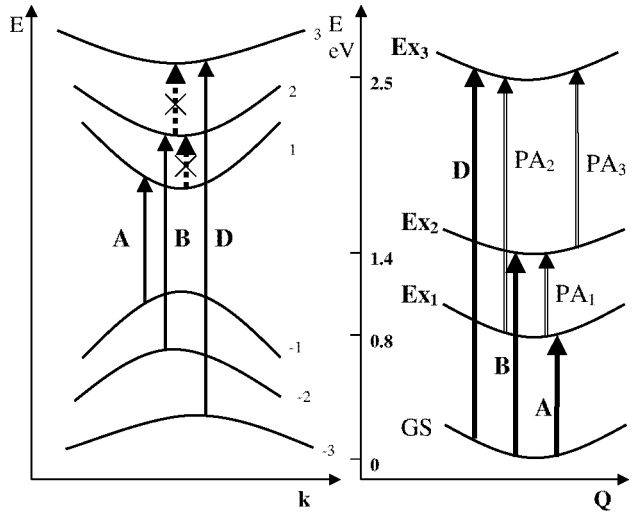

FIG. 2. Schematic representation of the excited states and optical transitions of S NT in the tight binding (a) and exciton picture (b), respectively. (a) The electron dispersion relation [$E(k)$] and the allowed interband optical transitions involving subbands with indices m of 1 to 3; optical transitions among subbands in the conduction or valence bands are *strictly forbidden*. (b) Various excitons (Ex_1 and Ex_2) in the NT configuration coordinate, Q, and their associated optical transitions from the ground state (GS) (A to D, full lines), and Ex_1 (PA_1 to PA_3, double lines).

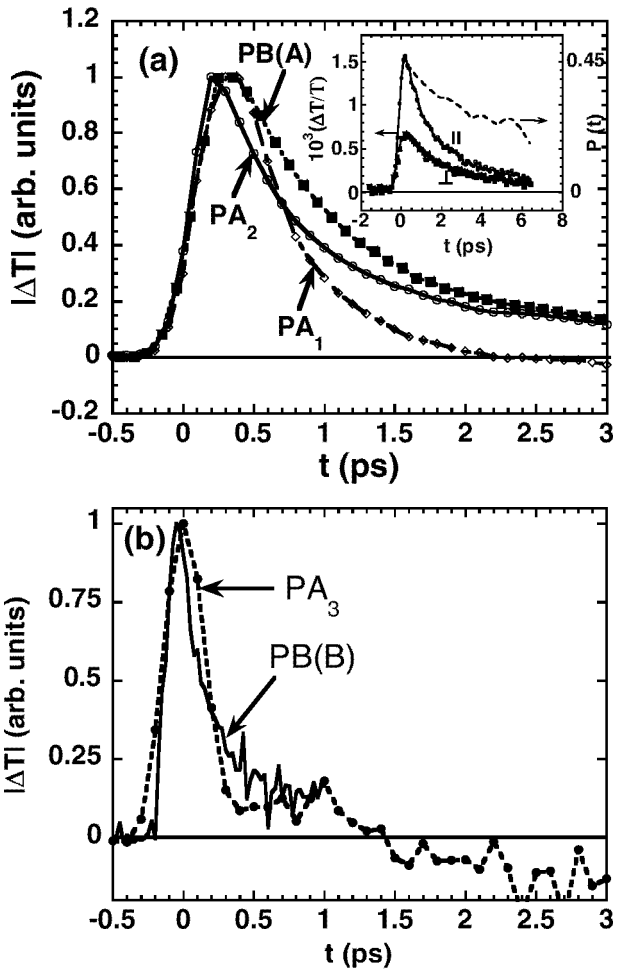

FIG. 3. Transient dynamics of various PA and PB bands in the PM spectrum of Fig. 1. (a) PB(A) and its associated PA_1 and PA_2 bands. (b) PB(B) and its associated PA_3. The inset in (a) shows $\Delta T(t)$ at 0.9 eV in parallel and perpendicular pump-probe polarizations, and the consequent polarization memory $P(t)$ decay.

background (Fig. 1). However, when examining the full PM spectrum obtained here (Fig. 1), we see that the PA spectrum does not agree with this interpretation [10], since it contains two well-resolved peaks (PA_1 and PA_2, respectively) and a threshold of another (PA_3). Moreover, the transient PA and PB are correlated, indicating that they share a common origin.

The transient dynamics of the various PA and PB bands in the PM spectrum are shown in Fig. 3. It is seen that, whereas PB(A) dynamics are similar to that of PA_1 and PA_2 [Fig. 3(a)] showing a lifetime of about 700 fs, PB(B) dynamics are correlated with that of PA_3 showing a lifetime of about 150 fs. In addition, the polarization memory dynamics $P(t)$ of PB(A) [Fig. 3(a) inset] also correlates with $P(t)$ of PA_1 and PA_2 bands (not shown). Moreover, from the initial $P(0)$ value of 0.45, we conclude that the PA and PB bands are polarized parallel to the NT axis. The correlation between the various PA and PB bands indicates that the PA bands should be associated with the primary photoexcitations in S NT, rather than with the global π plasmon [10]. It is noteworthy that photogenerated carriers in more common semiconductors do not show structured PA bands; instead their PA is in the form of a structureless Drude free carrier absorption that peaks at low energies [14]. In SWNTs, however, there is the possibility that the PA bands associated with the photogenerated carriers would show peaks that correspond to transitions between subbands, namely, electron (hole) transitions from m to $m + 1$ within the conduction (valence) subbands [Fig. 2(a)]. These optical transitions that are polarized along the NT are strictly forbidden in the tight binding model [1,15], since the angular momentum is not conserved. We therefore conclude that "free" charge carriers are not the primary photoexcitations in S NT.

Our results can be well explained, however, when e-h interaction [7–9] is taken into account. In this case, excitons are the primary excitations in S NT, where the e-h correlation leads to allowed optical transitions between subbands. The optical transitions of photoexcited exciton can be viewed in this picture as an electron promotion from $m = 1$ to higher m in the conduction subbands, and simultaneously a symmetric hole promotion from $m = 1$ to a lower valence subband with higher m. Such optical transitions are allowed since both linear and angular momenta are conserved; namely, $\Delta k = k_e - k_h = 0$, and $\Delta m = m_e - m_h = 0$. Simultaneously, energy is also conserved if the e-h binding energy is taken into account. A schematic representation of excitons and their optical transitions is given in Fig. 2(b). In this picture, bands A, B, and D are due to excitons, Ex_1, Ex_2, and Ex_3, respectively. Excitons in 1D have relatively large binding energy and "steal" most of the oscillator strength from the interband transition [5,7] explaining the large absorption strength of bands A, B, and D in S NT [7]. Moreover, PA bands such as PA_1 and PA_2 from Ex_1 and PA_3 from Ex_2 [see Fig. 2(b)] may be also formed. Our data can be well explained using the exciton picture: Excitation into band B creates Ex_2 that instantaneously forms PB(B) due to phase space filling and a correlated PA band (PA_3). Consequently, Ex_2 excitons decay within 150 fs [Fig. 3(b)] to the lower Ex_1 excitons that form PB(A) and two associated PA bands, PA_1 and PA_2, respectively, all having slower dynamics [Fig. 3(a)].

Further support for the exciton picture is provided by the polarization memory dynamics, $P(t)$ given in the Fig. 3(a) inset. We discovered that all transient PB and PA bands in the PM spectrum possess polarization memory, namely, $\Delta T_p(t) \neq \Delta T_{pe}(t)$ [Fig. 3(a) inset]. $P(t)$ decays within a few ps, and its dynamics are the same for each PB and its correlated PA bands. Photogenerated free carriers in SWNTs cannot have polarization memory that decays within several ps since they should be delocalized along the tube (that is not straight) very quickly following their generation at $t = 0$. The primary photoexcitations in the alternative model are excitons, confined in space within a few lattice constants. Because of this localization in space, such excitons would show polarization memory at $t = 0$, which may decay at $t > 0$ due to excitons diffusion along the NT. Similar photoinduced polarization memory and decay was seen before in quasi-1D conducting polymers, and, in particular, for photoinduced soliton pairs in fibrils of trans-$(CH)_x$ [16]; similarly, $P(t)$ was analyzed using soliton diffusion along the fibrils. $P(t)$ within this model is given by $P(t) = P(0)\exp(-4Dt/R^2)$, where D is the photoexcitation diffusion constant, and R is the average "radius of curvature" of the fibrils in the film. Using this "exciton diffusion along the NT" model to interpret the polarization memory decay in SWNTs, we calculate from $R = 300$ nm a diffusion constant $D \approx 120\ \mathrm{cm}^2/\mathrm{s}$ for the photogenerated excitons in S NTs.

Additional support for allowed intersubband transitions in S NTs is provided by the resonant multiphoton excitations seen in Fig. 4(a). The transient PM spectrum at $t = 0$ excited at 1 eV is shown at two different excitation intensities, $I = 300\ \mu\mathrm{J/cm}^2$ and $I = 1.5\ \mathrm{mJ/cm}^2$. In addition to the trivial PB(A) [17] (not shown here) and its relatively longer decay, we also see PB(B) at low I. Since band B lies higher than the excitation photon energy, then its photobleaching can be explained only by a two-photon-absorption (TPA) process into states at 1.6 eV [13]. However, to account for such a strong $\Delta T/T$ signal ($\approx$5%), the TPA process should be resonantly enhanced via an intermediate allowed state. A reasonable assumption for the TPA intermediate state is band A, whereas the final state is band B. This again suggests that A $\rightarrow$ B intersubband transition is allowed; consistent with the exciton model presented in Fig. 2(b).

The PM spectrum at high I [Fig. 4(a)] shows that PB(B) is gradually overwhelmed by another PA band, PA_x, whereas the photobleaching of band C (M NT) and band D (S NT) dramatically increase. We interpret PB(D) and its large value ($\approx$10%) as resonant three-photon absorption. Even though three-photon absorption

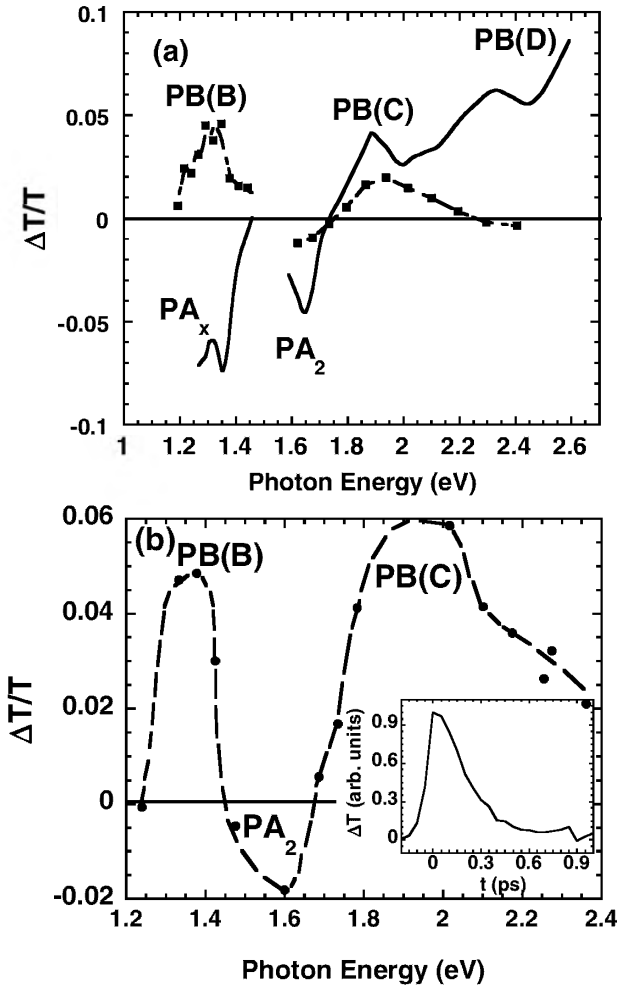

FIG. 4. Transient PM spectra at $t = 0$ excited at (a) 1 eV at two different pump excitation intensities, $I = 300\ \mu J/cm^2$ (squares) and $I = 1.5\ mJ/cm^2$ (solid line), and (b) at 2.0 eV. Various PB and PA bands are assigned. The inset in (b) shows the transient decay of PB(C) excited at 2.0 eV

is in general a very weak process, resonant three-photon absorption is apparently strong [18]. This process can be also viewed as sequential excitation via allowed intermediate states, namely $A \rightarrow B \rightarrow D$ showing that not only $A \rightarrow B$ transition, but also $B \rightarrow D$ transition is allowed.

The PM spectrum excited at 2 eV into band C (M NT) is shown in Fig. 4(b). Two PB bands are apparent; PB(B) of S NTs and PB(C) of M NTs. We note that PB(C) occurs either upon interband transition at 2 eV [Fig. 4(b)] or upon high-intensity excitation at 1 eV [Fig. 4(a)]. Since in M NTs there are no allowed optical transitions between 0.7 and 1 eV [1], we conjecture that PB(C) simply occurs by carrier heating [19]. This shows that the primary photoexcitations in M NTs are free carriers with extremely fast $P(t)$ decay (not shown here). At $t = 0$, these are "hot carriers," for which the electronic temperature T_e is not yet established; this explains the immediate appearance of PB(C) in the PM spectrum. Because of e-e collisions, the electron system reaches the quasiequilibrium state described by a temperature T_e, whereas most of the PM spectrum of M NTs occurs close to the Fermi energy [19]. This explains the ultrafast decay ($\approx$200 fs) of PB(C) [Fig. 4(b) inset]. PB(B) occurs in the PM spectrum [Fig. 4(b)] due to ultrafast intertube interaction in which photoexcitations can tunnel from M NTs into S NTs within the NT bundles, as well as due to direct photoexcitation of states with $Q \neq 0$ in S NTs [Fig. 2(b)] with subsequent relaxation to states with $Q \cong 0$.

We thank Dr. Efros and Dr. Garstein for important discussions. This work was supported in part by the NSF (DMR 02-02790) and the University of Utah; at University of Texas at Dallas, the work was supported by DARPA Grant No. MDA 972-02-C-005 and the Robert A. Welch foundation.

[1] M. S. Dresselhaus, G. Dresselhaus, and Ph. Avouris, *Carbon Nanotubes: Synthesis, Structures and Applications* (Springer-Verlag, Berlin, 2001).
[2] M. Bockrath *et al.*, Nature (London) **397**, 598 (1999).
[3] M. Pope and C. E. Swenberg, *Electronic Processes in Organic Crystals and Polymers* (Oxford University Press, New York, 1999), 2nd ed.
[4] S. Mazumdar and S. N. Dixit, Phys. Rev. Lett. **51**, 292 (1983).
[5] R. J. Eliott and R. Loudon, J. Phys. Chem. Solids **15**, 196 (1960).
[6] M. J. O'Connell *et al.*, Science **297**, 593 (2002); S. Bachilo *et al.*, Science **298**, 2361 (2002).
[7] T. Ando, J. Phys. Soc. Jpn. **66**, 1066 (1997).
[8] M. Ichida *et al.*, Phys. Rev. B **65**, 241407 (2002).
[9] C. L. Kane and E. J. Mele, Phys. Rev. Lett. **90**, 207401 (2003).
[10] J.-S. Lauret *et al.*, Phys. Rev. Lett. **90**, 57404 (2003).
[11] T. Pichler *et al.*, Phys. Rev. Lett. **80**, 4729 (1998), and references therein.
[12] H. Haug and S. W. Koch, *Quantum Theory and Electronic Properties of Semiconductors* (World Scientific, Singapore, 1990).
[13] S. Frolov *et al.*, Phys. Rev. Lett. **85**, 2196 (2000).
[14] J. I. Pankove, *Optical Processes in Semiconductors* (Dover, New York, 1971).
[15] A. Jorio *et al.*, Phys. Rev. Lett. **90**, 107403 (2003).
[16] Z. V. Vardeny *et al.*, Phys. Rev. Lett. **49**, 1657 (1982).
[17] M. Ichida *et al.*, Physica (Amsterdam) **323B**, 237 (2002).
[18] M. E. Brennan *et al.*, Opt. Lett. **28**, 266 (2003).
[19] T. Hertel and G. Moos, Phys. Rev. Lett. **84**, 5002 (2000).